University of
Strathclyde
Glasgow

Strathprints Institutional Repository

Ferguson, A. and Kelly, N.J. and Griffith, Brent and Weber, Andreas (2008) *Calibration and validation of a combustion-cogeneration.* In: The Canadian Building Simulation Conference, eSim 2008, 2008-05-20 - 2008-05-22, Quebec City, Canada.

http://strathprints.strath.ac.uk/

CALIBRATION AND VALIDATION OF A COMBUSTION-COGENERATION MODEL

Alex Ferguson[1], Nick Kelly[2], Andreas Weber[3], Brent Griffith[4]

[1] CANMET Energy Technology Centre, Natural Resources Canada, Ottawa
[2] Energy Systems Research Unit, University of Strathclyde, Glasgow, UK
[3] Swiss Materials Science and Technology Labs (Empa), Dübendorf
[4] National Renewable Energy Laboratory (NREL), Golden, USA

ABSTRACT

This paper describes the calibration and validation of a combustion cogeneration model for whole-building simulation. As part of IEA Annex 42, we proposed a combustion cogeneration model for studying residential-scale cogeneration systems based on both Stirling and internal combustion engines. We implemented this model independently in the EnergyPlus, ESP-r and TRNSYS building simulation programs, and undertook a comprehensive effort to validate the model's predictions. Using established comparative testing and empirical validation principles, we vetted the model's theoretical basis and its software implementations. The results demonstrate acceptable-to-excellent agreement, and suggest the calibrated model can be used with confidence.

INTRODUCTION

Today, decentralized cogeneration systems are an attractive alternative to traditional, centralized electrical supply. By exploiting the simultaneous electric and thermal output of cogeneration devices, overall efficiencies greater than 90% (based on the lower heating value, LHV) can be achieved. If managed carefully, these systems also deliver economic savings and greenhouse gas emission reductions. (Knight and Ugursal, 2005)

Recognizing the importance of modelling these systems, the International Energy Agency (IEA) approved the formulation of a new research annex (Annex 42) under the Energy Conservation in Buildings and Community Systems (ECBCS) implementing agreement. Key objectives of Annex 42 included the development and validation of simulation models for building-integrated fuel cell, Stirling, and internal combustion based cogeneration systems, and the comparison of these systems in different case studies.[1]

Over the last four years, Annex 42 developed and refined an empirical model suitable for modelling both Stirling engine (SE) and internal-combustion engine (ICE) cogeneration systems in a whole-building simulation context. This model is now implemented in three publicly available building simulation programs: EnergyPlus, ESP-r and TRNSYS.

Our work has progressed considerably since Ferguson and Kelly (2006) last reported on the these activities; Annex 42 undertook a broad validation effort guided by the principles put forth by Judkoff and Neymark (1995). This effort vetted all three model implementations, and compared predictions to test results for residential cogeneration equipment recently collected by other Annex 42 participants.

This paper describes these developments. First, we review relevant portions of the combustion cogeneration model, and discuss methods to validate the model. Next, we describe the inter-model comparative testing of the three model implementations. Finally, we discuss calibration and validation of the model using the experimental data collected within Annex 42.

COMBUSTION COGENERATION MODEL

Early in its working phase, Annex 42 recognized that the detailed measurements required by high-resolution ICE and SE models are unlikely to be available for production cogeneration equipment. While individual components (for example, an alternator) within these devices contribute to the performance of the entire system, the data required to meaningfully model these components is scarce. For this reason, Annex 42 developed parametric models that aggregate large components of the cogeneration system into control volumes, and use empirical correlations to characterize the energy flows into and out of these control volumes.

As described in Beausoleil-Morrison and Kelly (2007, Section III), the resulting combustion cogeneration model pared down the model resolution to the minimum necessary to study the device's response to building loads and conditions in the mechanical plant. The behaviour of subsystems that affect engine performance but do not directly interact with other components within the building were aggregated into parametric, energy conversion correlations. The system's dynamic characteristics were accounted for by coupling the steady-state model to a lumped-parameter thermal model.

The combustion cogeneration model comprises three control volumes, which are depicted in Figure 1:

---

[1]The website www.cogen-sim.net provides more information on Annex 42's activities, as well as copies of Annex 42 publications.
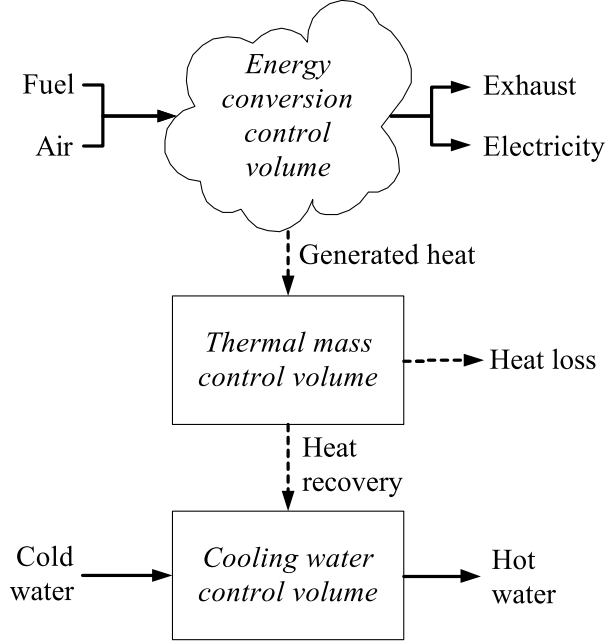
Figure 1: Control volume topology

The **energy conversion control volume** characterizes the steady-state rate of energy conversion in the device.

The **thermal mass control volume** aggregates the thermal mass of the engine and, in the case of SE-based units, auxiliary systems such as the blower and heater.

The **cooling water control volume** aggregates the engine cooling water, and encapsulating engine cooling-jacket and exhaust-gas heat exchangers.

Energy conversion control volume

The energy conversion control volume characterizes the steady-state conversion of fuel to heat and electricity. The model does not solve the energy balance for the energy conversion control volume. Instead, it calculates the rates of heat and power generation using overall electrical and thermal energy conversion efficiencies that aggregate the effects of incomplete combustion, friction and vibration, and energy use by auxiliary systems:

$$q_{gross} = \dot{m}_{fuel} \cdot LHV_{fuel} \qquad (1)$$
$$P_{net,ss} = \eta_{p,net} q_{gross} \qquad (2)$$
$$q_{gen} = \eta_{q,gross} q_{gross} \qquad (3)$$

where q_{gross} is the gross heat input into the system, $P_{net,ss}$ is the steady-state net electrical output, q_{gen} is the rate of steady-state gross heat generation. Symbol $\eta_{p,net}$ is

the unit's net electric efficiency, while symbol $\eta_{q,gross}$ is the unit's gross thermal efficiency. Finally, $\dot{m}_{fuel}$ is the system fuel flow rate, and LHV_{fuel} is the lower heating value of the fuel.

The model correlates the system's steady-state electrical and thermal efficiencies to the flow rate and inlet temperature of cooling water ($\dot{m}_{cw}$ and $T_{cw,i}$), and the gross heat input (q_{gross}) to the system:

$$\eta_{p,net} = a_0 + a_1(q_{gross}) + a_2(q_{gross})^2 \qquad (4)$$
$$+ a_3(\dot{m}_{cw}) + a_4(\dot{m}_{cw})^2$$
$$+ a_5(T_{cw,i}) + a_6(T_{cw,i})^2$$

$$\eta_{q,gross} = b_0 + b_1(q_{gross}) + b_2(q_{gross})^2 \qquad (5)$$
$$+ b_3(\dot{m}_{cw}) + b_4(\dot{m}_{cw})^2$$
$$+ b_5(T_{cw,i}) + b_6(T_{cw,i})^2$$

where a_0–a_6 and b_0–b_6 are empirical coefficients.

The model does not explicitly consider the heat transfer to the cooling water in the system's exhaust gas heat exchanger. Instead, it aggregates these effects into the overall thermal efficiency coefficient (η_q). This approach reduces the complexity of the model and introduces some error, but the experiments conducted within Annex 42 did not include the invasive instrumentation necessary to separately characterize the engine-jacket and exhaust-gas heat transfer. The correlations in Equations 4 and 5 can be calibrated without separately measuring the engine jacket and exhaust-gas heat transfer.

Thermal mass control volume

The model lumps the thermal mass associated with the engine into a single, homogeneous control volume. The thermal energy stored within the thermal mass control volume is quantified using an aggregate thermal mass ($[MC]_{sys}$) and an average temperature (T_{sys}).

The rate of heat transfer between the thermal mass and cooling water control volumes is proportional to the temperature difference between these control volumes:

$$q_{HX} = UA_{HX}(T_{sys} - T_{cw,o}) \qquad (6)$$

where q_{HX} is the rate of heat recovery, UA_{HX} is the overall heat transfer coefficient between the control volumes, and T_{sys} and $T_{cw,o}$ are the average temperatures within the control volumes.

The rate of heat loss to the room is:

$$q_{loss} = UA_{loss}(T_{sys} - T_{room}) \qquad (7)$$

where q_{loss} is the rate of heat loss, UA_{loss} is the coefficient of heat loss, and T_{room} is the temperature in the surrounding enclosure.

Finally, the energy balance in the thermal mass control volume is:

$$[MC]_{sys}\frac{dT_{sys}}{dt} = q_{gen} - q_{HX} - q_{loss}$$
$$= q_{gen} - UA_{HX}(T_{sys} - T_{cw,o})$$
$$- UA_{loss}(T_{sys} - T_{loss}) \qquad (8)$$

where $[MC]_{sys}$ and T_{sys} are the effective heat capacitance and the average temperature of the thermal mass control volume, respectively.

Cooling water control volume

Both the exhaust-gas heat exchanger and the engine cooling jacket transfer heat to the cooling water. The energy balance in the cooling water control volume is:

$$[MC]_{HX}\frac{dT_{cw,o}}{dt} = [\dot{m}C_p]_{cw}(T_{cw,i} - T_{cw,o}) \qquad (9)$$
$$- UA_{HX}(T_{cw,o} - T_{sys})$$

where $[MC]_{HX}$ is the total thermal capacitance of the control volume including the cooling water and encapsulating heat exchangers, and $\dot{m}_{cw}$ and $C_{p,cw}$ are the cooling water flow rate and specific heat capacity. $T_{cw,i}$ and $T_{cw,o}$ are the cooling water temperatures at the inlet and outlet of the cooling water control volume.

Finally, the actual rate of heat recovery (q_{rec}) from the cogeneration unit is:

$$q_{rec} = [\dot{m}C_p]_{cw}(T_{cw,o} - T_{cw,i}) \qquad (10)$$

VALIDATION METHODS

Judkoff and Neymark (1995) classified error sources in building simulation programs into three groups: i) differences between the simplified model and the actual physical processes occurring in the system, ii) errors or inaccuracies in the mathematical solution of the models, and iii) coding errors. They also proposed a pragmatic, three-step approach to identify these errors:

Comparative testing compares the predictions of one program to those obtained from other programs using similar boundary conditions.

Analytical validation compares a program's predictions to a known analytical solution for a simple problem that isolates one part of the model.

Empirical validation compares a program's predictions to monitored data collected for a real system under laboratory or field conditions.

A general principle applies to all three steps—the simpler and more controlled the test case, the easier it is to identify and diagnose sources of error. Realistic cases may help test the interactions between algorithms, but are less useful for identifying and diagnosing errors. Comparison of the actual long-term energy usage of a building with simulation results may best convince a building designer that a program is valid, but this is actually the least conclusive test. The simultaneous operation of all possible error sources combined with the possibility of offsetting errors means that good or bad agreement cannot be attributed to program validity.

Annex 42 did not employ analytical validation due to the complex nature of cogeneration devices and the lack of appropriate analytic solutions for the relevant thermodynamic processes. The remaining two steps, empirical validation and comparative testing, were applied to vet the combustion cogeneration model.

COMPARATIVE TESTING

Comparative testing consists of exercising all three model implementations (EnergyPlus, ESP-r and TRNSYS) using equivalent inputs and boundary conditions. While disagreement in the results suggests an error in one (or all) of the programs, agreement between the programs does not guarantee the three implementations are error-free. Though all of the simulation programs may produce similar results, all may be incorrect.

We devised an inter-model comparative test suite for the combustion cogeneration model. Comprising 44 test cases, this test suite exercises most of the source code in the EnergyPlus, ESP-r and TRNSYS implementations. By design, the test cases make no attempt to represent realistic cogeneration systems or operational configurations. Rather, they are intended to exercise specific aspects of the model and to exaggerate differences between implementations for the purposes of diagnosing errors.

Comparative testing uncovered numerous differences between the predictions made by the model's three initial implementations. Not all of these stemmed from source code errors (that is, bugs); several aspects of the model were misinterpreted by the implementation authors, and in some cases the solution philosophies used in the respective simulation programs introduced differences into the results. Over the course of the testing programme, we identified and corrected numerous errors in each of the implementations. All three now reliably produce comparable predictions.

Beausoleil-Morrison and Ferguson (2008, Section III) describe the test suite and the accompanying results in detail; Figure 2a depicts the results of one such test. Test case 307 subjects the combustion cogeneration model to a constant electrical load for the first hour of the test, and then deactivates the model for the remainder of the simulation. ESP-r predicted higher engine temperatures than TRNSYS, and careful review of the two implemen-
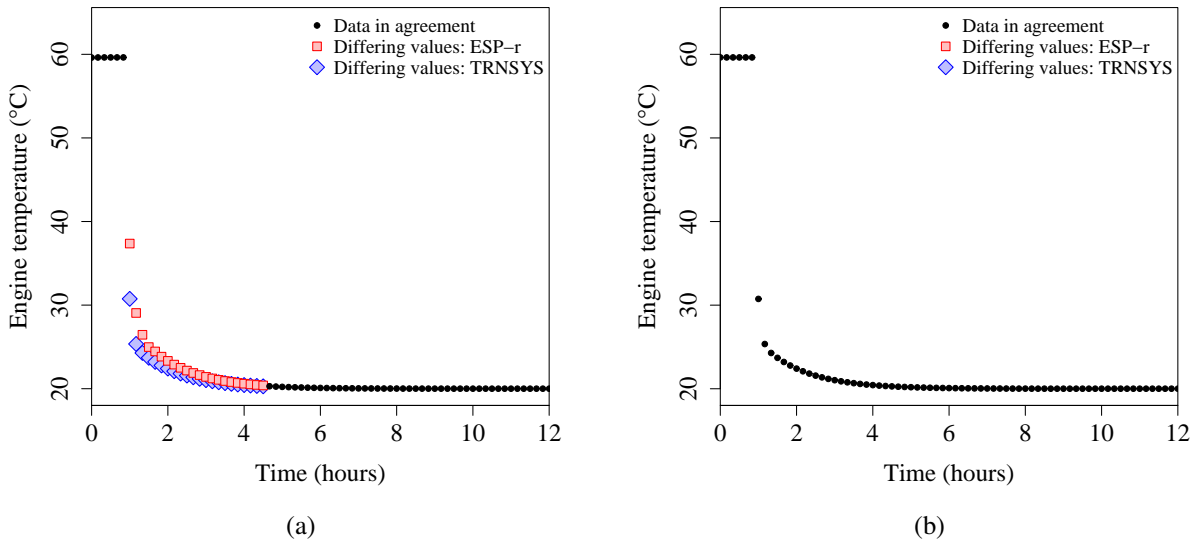
Figure 2: Comparison of predicted engine temperature with a) ESP-r bug, and b) ESP-r bug fixed

tations uncovered an error in the ESP-r procedure.

ESP-r uses forward- and backward-difference approximations of the model's state-space equations (Equations 8 and 9) to estimate the state variables (that is, T_{sys} and $T_{cw,o}$) on the next time-step. By default, ESP-r uses the Crank-Nicholson solution scheme, and assigns equal weight to the forward- and backward-difference terms. When ESP-r judges the Crank-Nicholson scheme to be unstable, it switches to a fully-implicit formulation and the solution is determined entirely using the forward-difference terms. (Clarke, 2001)

The ESP-r implementation of the Annex 42 model incorrectly applied the stability criteria, causing the model to conclude the Crank-Nicholson solution was stable when it in fact was not. Once the ESP-r implementation was corrected, the two implementations agreed exactly (see Figure 2b).

EXPERIMENTAL TESTS

In 2004, annex participants defined an experimental protocol for testing cogeneration equipment. This protocol guided Annex 42 testing programs to ensure the resulting data were suitable for calibration and validation of the annex models. The protocol prescribes the instrumentation and test regimes necessary to fully characterize a cogeneration device's performance in the context of building simulation. Beausoleil-Morrison (2008, Section II) describes the protocol in detail.

We calibrated and validated the combustion cogeneration model using results from two Annex 42 experimental studies:

- In 2003, The Canadian Centre for Housing Technology (CCHT) evaluated a SE cogeneration device (700 W electric, 7 kW thermal) in a test house in Ottawa.

- In 2006, Forschungsstelle für Energiewirtschaft (FfE) installed an ICE cogeneration unit (5.5 kW electric, 12.5 kW thermal) on a laboratory test rig in Munich.

Beausoleil-Morrison (2008, Sections III and IV) describes these two facilities and the experiments conducted there. Though they considered different technologies, the results from the two test programs pose similar challenges for calibration and validation.

The CCHT experiments commenced prior to establishment of the Annex 42 experimental protocol and, for this reason, employed none of the invasive instrumentation prescribed by the protocol. While FfE adhered to the protocol as closely as possible, FfE's agreement with the ICE manufacturer precluded invasive instrumentation. Thus, both the CCHT and FfE datasets describe only the energy and mass flows entering and leaving the cogeneration devices; they contain no measurements of conditions inside the devices.

The CCHT study installed the SE device inside a test house, and operated the device in response to the real heating loads of that building. Though FfE tested the ICE device on a laboratory bench, this apparatus was designed specifically to recreate conditions inside a residence as realistically as possible. Thus, neither the CCHT nor the FfE facilities could impose steady-state

conditions (that is, constant inlet cooling water temperatures) on the devices, and all of the data from these studies describe the systems' dynamic response to changing conditions.

The CCHT dataset used by Annex 42 comprises 164 hours of measurements collected over three separate intervals. One of these intervals, totalling 67 hours, was used for model calibration work, while the remaining data were used for validation purposes.

Likewise, the FfE data comprises 72 hours of measurements, collected in three separate, 24-hour periods. One of these periods was used to calibrate the Annex 42 model, while the remaining periods were reserved for validation. Validation using the FfE data was not undertaken within Annex 42, but the data are available for future efforts.

CALIBRATION

While neither the CCHT nor FfE results are optimally-suited for Annex 42's work, they still provide a rich, high-resolution description of emerging SE- and ICE-based cogeneration technology under realistic operating conditions. Their relevance to current technology, and their availability to Annex 42, recommended their use in the Annex's calibration and empirical validation work.

Beausoleil-Morrison (2008, Sections V and VI) provides a comprehensive description of these calibration efforts. Below, we focus on strategies for coping with the key challenge associated with the FfE and CCHT datasets—the lack of invasive measurements, and steady-state tests.

Dynamic Parameter Estimation

Calibration of the Annex 42 models required derivation of key model parameters from a handful of measurements of the energy and mass flows entering and leaving the cogeneration unit. These measurements describe:

- the fuel flow rate

- the rate of net electric output

- the cooling water flow rate

- the cooling water temperature

- the ambient temperature

The CCHT and FfE dynamic test regimes further complicated this task; only dynamic measurements were available for calibrating both the steady-state (η_p and η_q) and dynamic ($[MC]_{eng}$, $[MC]_{HX}$, UA_{HX} and UA_{loss}) parameters. For these reasons, we adopted a non-traditional calibration strategy; instead of estimating each of the input parameters individually, we estimated all six parameters simultaneously using an iterative approach:

1. A set of input parameters was chosen.

2. The model was subjected to the same cooling water temperature and flow rate, enclosure temperature and control signals as the cogeneration units studied in the CCHT and FfE tests.

3. The model's predicted outlet temperature, fuel flow rate and power generation were compared each measurement in the CCHT and FfE datasets, and the errors in the model's estimates were quantified.

4. The model inputs were adjusted, and steps 2–4 were repeated until the best-possible agreement between model outputs and empirical data was achieved (that is, errors between measurements and estimates were minimized).

Clearly, this procedure is computationally intensive and may many iterations. To expedite the search for the input parameters, we employed third-party optimization utilities developed by Eldred et al. (2006) and Wetter (2004) that were specifically designed for coupling with simulation programs. These utilities automated steps 2–4 of the parameter identification process, and performed thousands of simulations while searching for the optimal input set. They also employ suites of single- and multi-objective optimization algorithms to quickly converge on the most suitable input values.

(Beausoleil-Morrison, 2008, Sections V and VI) describe application of these utilities in detail. The coupling between the optimization utility and the combustion cogeneration model is depicted in Figure 3. During each iteration, the utility wrote the estimated model parameters to the building simulation program's input files. The utility then invoked the building simulation program, which performed a simulation using the parameters described in the input files and the measured boundary conditions. The building simulation program wrote the results to an output file. Finally, the utility interpreted the simulator's output and selected new values for the parameters based on the results of the simulation according to the selected optimization algorithm.

These optimization programs were designed to determine the parameter set providing the minimum values for a given criteria (called a *cost function*). Three cost functions were defined to describe the accuracy of the model's predicted fuel flow, electrical and thermal output. For example, the cost function describing the error in the net power generation is:

$$\bar{c}_p = \frac{\sum_{i=1}^{n} (P_{net,model} - P_{net,measured})_i^2}{(P_{net,\max} - P_{net,\min})} \quad (11)$$

where $\bar{c}_p$ is the cost function result describing error in the model's predictions of power output. $P_{net,model}$ and $P_{net,measured}$ describe the predicted and observed power
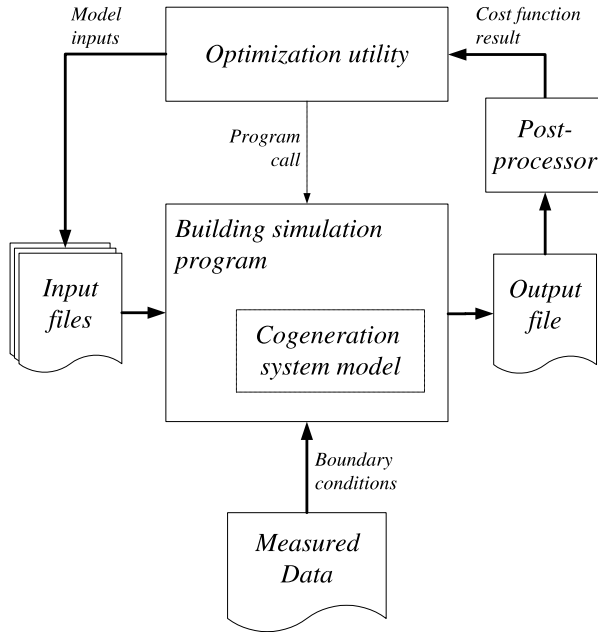
Figure 3: Parameter identification schematic

Table 1: Calibrated parameters for SE and ICE devices

Parameter	Units	SE	ICE
$[MC]_{eng}$	J/°C	18.5×10^3	63.6×10^3
$[MC]_{HX}$	J/°C	28.1×10^3	1.00×10^3
UA_{HX}	W/°C	31.8	741
UA_{loss}	W/°C	4.64	13.7
a_0	–	0.0929	0.27
b_0	–	0.970	0.66

generation at time step i, while $P_{net,\max}$ and $P_{net,\min}$ describe the maximum and minimum power output observed over the dataset.

The steady-state net-power and gross-heat generation efficiency equations (Equations 4 and 5) correlate the unit's energy conversion efficiency to the operating point (q_{gross}), the cooling water flow rate ($\dot{m}_{cw}$), and inlet temperature ($T_{cw,o}$). But the unit's sensitivity to all of these factors could not be quantified for three reasons:

- Neither the SE unit tested at CCHT, nor the ICE unit tested at FfE were designed to modulate, and both devices operated at a single operating point throughout the tests.

- The CCHT test apparatus supplied the SE unit with cooling water at a constant flow rate. Though the FfE tests varied the flow rate, inspection of the results indicated no sensitivity to these changes.

- While the thermal output of the SE and ICE units is likely sensitive to the cooling water temperature, both the CCHT and FfE datasets contain few measurements with cooling water inlet temperatures below 50 °C. In the remaining measurements, the cooling water is likely too warm to affect significant condensation in the exhaust gas heat exchanger. Under these conditions, the units' performance is insensitive to cooling water temperature.

For these reasons, the empirical polynomials describing the unit's electric and thermal efficiencies were reduced to constant values (that is, $\eta_{p,net} = a_0$ and $\eta_{q,gross} = b_0$).

It is unfortunate that we do not have better descriptions of the SE and ICE units' sensitivity to the cooling water temperature, which will undoubtedly affect thermal output. But the results of the CCHT and FfE tests illustrate an important point: when integrated into into real houses, cogeneration equipment may spend much its time in non-condensing operation. These units will not achieve the high thermal efficiencies possible with condensing heat exchange, and the CCHT and FfE studies provide a more realistic appraisal of performance.

Calibration Results

The key model parameters computed for both the ICE and SE units are presented in Table 1. At first glance the SE unit's net electrical efficiency (a_0) is surprisingly low; this reflects the high heat-to-power ratio of this unit (approximately 10:1). And while the SE unit's gross heat generation efficiency (b_0) is nearly 100%, this parameter describes the total heat generation within the device, and does not account for heat lost to the surroundings.

Comparison of the predictions with the calibration datasets suggests that the parameters well-represent the SE and ICE units. For instance, Figure 4 compares the predicted outlet temperatures with their corresponding measurements. To further assess the model's accuracy, we undertook a quantitative validation study using the CCHT dataset.

EMPIRICAL VALIDATION

To evaluate the accuracy of the calibrated model, we compared its predictions to the measurements in the remaining 93 hours of the CCHT dataset. This step is an important test for the Annex 42 model—whereas comparative testing merely identifies bugs within the model, empirical validation assesses the model's suitability for representing real cogeneration systems.

Comparison Metrics

Four metrics quantify the accuracy of the combustion cogeneration model: i) the average absolute error, ii) the maximum absolute error, ii) the root mean square error,
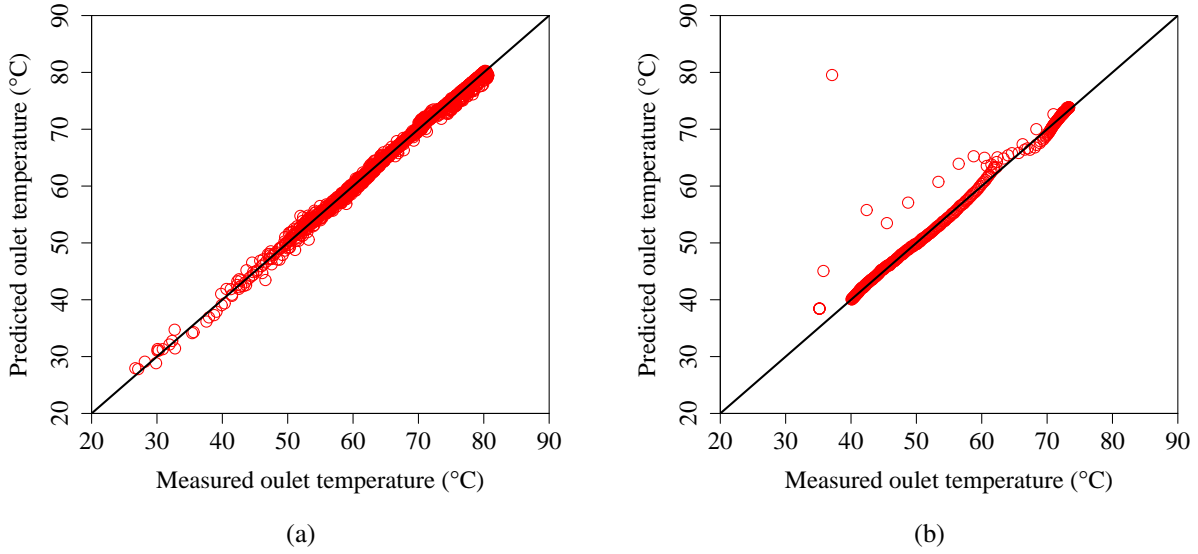
Figure 4: Results of calibration using (a) CCHT SE and (b) FfE ICE datasets

and iv) the correlation coefficient.

The average ($\bar{e}_{\text{abs}}$) and maximum absolute ($\bar{e}_{\text{abs,max}}$) errors are:

$$\bar{e}_{\text{abs}} = \frac{1}{n}\sum_{i=1}^{n}|\hat{\theta}_i - \theta_i| \qquad (12)$$

$$e_{\text{abs,max}} = \max\left(\{|\hat{\theta}_i - \theta_i|\}_{i=1}^{n}\right) \qquad (13)$$

where n is the number of measurements, and $\hat{\theta}_i$ and θ_i are the measured and predicted values at time step i.

The root mean square error (e_{RMS}) is:

$$e_{RMS} = \sqrt{\frac{1}{n}\sum_{i=1}^{n}(\hat{\theta}_i - \theta_i)^2} \qquad (14)$$

and the correlation coefficient is calculated as follows:

$$r^2 = \frac{\sum_{i=1}^{n}\left[\left(\hat{\theta}_i - \bar{\hat{\theta}}\right)(\theta_i - \bar{\theta})\right]}{\sqrt{\sum_{i=1}^{n}\left[\left(\hat{\theta}_i - \bar{\hat{\theta}}\right)^2(\theta_i - \bar{\theta})^2\right]}} \qquad (15)$$

where:

$$\bar{\hat{\theta}} = \frac{1}{n}\sum_{i=1}^{n}\hat{\theta}_i, \text{ and } \bar{\theta} = \frac{1}{n}\sum_{i=1}^{n}\theta_i$$

Validation results

The model exhibited acceptable-to-excellent agreement with the CCHT measurements. Table 2 presents the comparison metrics quantifying the error in the predicted fuel flow rate, net power output, heat recovery and the cooling water outlet temperature. While the maximum observed error suggests non-trivial differences between the measurements and predictions (for instance, the maximum error in heat recovery is approximately 40% of the maximum observed rate of heat recovery), these errors persisted for a single time step, and always occurred at the start of the cogeneration unit's operating cycle. As the average- and RMS-error, and correlation coefficient data indicate, the model agreed well with measurements throughout the remainder of the simulation.

Moreover, the model's predictions of cumulative fuel consumption, electricity generation, and heat recovery also agreed well with measurements. At the end of 93 hours of simulation, the predicted fuel consumption differed from measurements by 0.34%, the predicted electricity generation differed by 3.1%, and the predicted heat recovery differed by 1.7%.

As with all validation efforts, uncertainty associated with the CCHT data and the calibration of the model using these data diminish the confidence with which the model can be validated. Of all the sources of uncertainty, perhaps the hardest to quantify is that associated with the calibration procedure. Because optimization tools were specifically employed to minimize the error between predictions and measurements, they may have inadvertently selected input values that compensate for logical or coding errors in the model. Therefore, the model's underlying principles and its implementation in computer code cannot be rigorously validated when using the input parameters derived from the CCHT data.

Nevertheless, when calibrated using the inputs derived from the CCHT data, the model is clearly an accurate representation of the cogeneration unit tested at CCHT.

Table 2: Comparison of combustion cogeneration model and CCHT measured data

Parameter	Units	$\bar{e}_{abs}$	$e_{abs,max}$	e_{RMS}	r^2
Fuel flow rate ($\dot{m}_{fuel}$)	kg/s	0.604×10^{-6}	13.5×10^{-6}	1.82×10^{-6}	1.00
Net electric output (P_{net})	W	16.4	124	29.6	0.993
Rate of heat recovery (q_{rec})	W	69.5	2940	218	0.991
Outlet temperature ($T_{cw,o}$)	°C	0.280	3.36	0.471	0.991

CONCLUSIONS

In support of Annex 42's research objectives, we developed a model for studying combustion-based cogeneration equipment in whole-building simulation. The combustion cogeneration model is parametric in nature, and pares down the system complexity to the minimum required to meaningfully study the interactions between a cogeneration system and the building.

We implemented the model in three publicly-available building simulation programs (EnergyPlus, ESP-r and TRNSYS), and vetted all three implementations by extensively comparing their predictions. All three implementations produce similar results, and we are confident they faithfully represent the Annex 42 model.

We calibrated and validated the model using data collected by CCHT and FfE. Though these experiments provided a rich description of cogeneration system performance, they do not include the steady-state tests or invasive instrumentation required for the Annex's calibration and validation research.

These limitations necessitated a non-traditional calibration procedure—using optimization tools, we selected a set of model inputs providing the best agreement with measurements. The resulting inputs provide good-to-excellent agreement, suggesting the model, as calibrated in this study, can be used with confidence.

Since completion of this work, FfE and other annex participants have tested additional combustion cogeneration equipment. We are confident that data from these tests will allow improved calibration and validation of the Annex 42 combustion model in the future.

ACKNOWLEDGEMENTS

REFERENCES

Beausoleil-Morrison, I., ed. (2008), *Experimental Investigation of Residential Cogeneration Devices and Calibration of Annex 42 Models*, IEA/ECBCS Annex 42. Available at www.cogen-sim.net.

Beausoleil-Morrison, I. and Ferguson, A., eds (2008), *Inter-model Comparative Testing and Empirical Validation of Annex 42 Models for Residential Cogeneration Devices*, IEA/ECBCS Annex 42. Available at www.cogen-sim.net.

Beausoleil-Morrison, I. and Kelly, N., eds (2007), *Specifications for Modelling Fuel Cell and Combustion-Based Residential Cogeneration Device within Whole-Building Simulation Programs*, IEA/ECBCS Annex 42. Available at www.cogen-sim.net.

Clarke, J. (2001), *Energy simulation in building design*, second edn, Butterworth Heinemann.

Eldred, M., ed. (2006), *DAKOTA, A Multilevel Parallel Object-Oriented Framework for Design Optimization, Parameter Estimation, Uncertainty Quantifcation, and Sensitivity Analysis: Version 4.0 reference manual*, Sandia National Laboratories.

Ferguson, A. and Kelly, N. (2006), Modelling Building Integrated Stirling CHP Systems, *in* 'Proceedings of eSim 2006 Building Performance Simulation Conference', International Building Performance Simulation Association.

Judkoff, R. and Neymark, J. (1995), *International Energy Agency Building Energy Simulation Test (BESTEST) and Diagnostic Method*, IEA/ECBCS Annex 21 and IEA/SHC Task 12. NREL/TP-472-6132.

Knight, I. and Ugursal, I., eds (2005), *Residential Cogeneration Systems: A Review of the Current Technologies*, IEA/ECBCS Annex 42. Available at www.cogen-sim.net.

Wetter, M. (2004), *GenOpt: Generic Optimization Program*, Lawerance Berkeley National Laboratory, US Deparment of Energy. User manual.